Magnetic hardening studies in sintered $Sm(Co,Cu_x,Fe,Zr)_z$ 2:17 high temperature magnets

Yong Zhang,[a] Michelle Corte-Real, and George C. Hadjipanayis
Physics and Astronomy Department, University of Delaware, Newark, Delaware 19716

Jinfang Liu and Marlin S. Walmer
Electron Energy Corporation, Landisville, Pennsylvania 17538

Kannan M. Krishnan
Lawrence Berkeley National Laboratory, Berkeley, California 94720

Lorentz microscopy combined with conventional transmission electron microscopy were used to image the magnetic domains and microstructures of sintered $Sm(Co_{bal}Cu_xFe_{0.06}Zr_{0.03})_z$ ($0.088 \leqslant x \leqslant 0.128$; $5.8 \leqslant z \leqslant 7.2$) permanent magnets which were specifically designed for high temperature applications. The microstructural data were correlated with the magnetic measurements to understand the origin of coercivity. All sintered magnets showed typical cellular and lamellar microstructures. The cell size and coercivity were found to be more sensitive to *z* than to the Cu content. For a fixed Cu content, by increasing *z* from 5.8 to 7.2, the cell size was found to vary dramatically from 10 to 80 nm and the coercivity from 5.6 to 40 kOe, respectively. On the other hand, for fixed *z*, the cell size decreases slightly with increasing Cu content from 0.08 to 0.128 and the corresponding coercivity increases from 23.6 to 40 kOe. Both *z* and the Cu content show a smaller effect on the cell boundary width and lamella phase density. Domain wall pinning is observed in all magnets studied, irrespective of their cell size. The smaller the cell size, the less wavy the walls are, and the lower the coercivity. The Lorentz microscopy data indicate that the majority of pinning sites are the cell boundaries with occasional pinning at the intersection of cell boundaries with the lamella phase.
[S0021-8979(00)29208-6]

I. INTRODUCTION

Precipitation hardened Sm–(Co,Cu,Fe,Zr) magnets, with the highest Curie temperature among the commercial rare-earth permanent magnets, are the most promising candidates for the Department of Defense's high temperature applications. It has been established that the coercivity mechanism of Sm–(Co,Cu,Fe,Zr) magnets is of domain wall pinning type.[1–5] The $Sm_2(Co,Fe)_{17}$ cells are responsible for the saturation magnetization, while the $Sm(Co,Cu)_5$ cell boundaries pin the domain walls.[1] The Zr-rich lamella phase is believed to provide diffusion paths for Cu segregation, thus helping to form a uniform $Sm(Co,Cu)_5$ cell boundary phase, which then leads to high coercivity.[3] However, some other pinning sites in $Sm(Co,Cu,Fe,Zr)_z$ magnets besides the 1:5 cell boundaries were reported in recent years.[4,6,7] Katter *et al.*[7] theoretically proposed a new pinning site as the intersection between cell boundaries and the lamella phase which according to them was stronger than that at the edge of cell boundaries. This mode, however, was never confirmed by Lorentz microscopy.

Although extensive studies were done on Sm(Co,Cu, Fe,Zr) 2:17 magnets in the past few decades, there is lack of a systematic study on the magnetic hardening mechanism, especially using Lorentz microscopy to investigate the possible domain wall pinning sites. In this article, Lorentz microscopy combined with conventional transmission electron microscopy (TEM) were used to image the magnetic domains and microstructures of magnets with different Cu contents and ratio *z* values. The microstructural data were correlated with coercivity in order to understand the magnetic hardening mechanism.

II. EXPERIMENTAL MATERIALS AND PROCEDURE

The $Sm(Co_{bal}Cu_xFe_{0.06}Zr_{0.03})_z$ ($0.088 \leqslant x \leqslant 0.128$; $5.8 \leqslant z \leqslant 7.2$) permanent magnets were sintered at 1220 °C, solubilized at 1205 °C, and then heat treated at 790 °C for up to 36 h followed by slow cooling at 0.7 °C/min to 400 °C. All TEM samples were cut perpendicular and parallel to the *c* axis, respectively, and mechanically polished before being

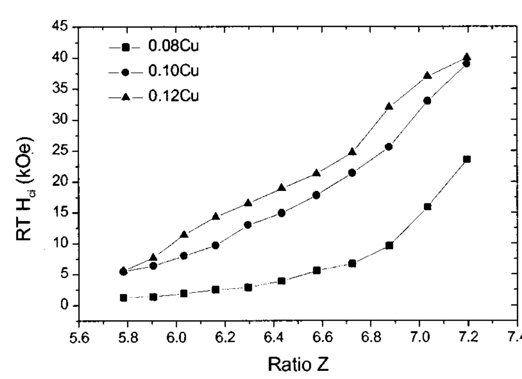

FIG. 1. Dependence of room temperature coercivity H_{ci} on ratio *z* for the sintered $Sm(Co_{bal}Cu_xFe_{0.06}Zr_{0.03})_z$ magnets ($x = 0.08$, 0.10, and 0.12).

[a]Corresponding author; electronic mail: yzhang@physics.udel.edu

thinned by ion milling. Conventional TEM was carried out on a JEOL JEM-2000FX at 200 kV. Fresnel and Foucault mode Lorentz microscopy was run on a JEOL JEM-100CX at 100 kV and on a Philips CM20 with 200 kV. The room temperature magnetic properties were measured using an Oxford vibrating sample magnetometer (VSM) with a maximum applied field of 50 kOe and with a superconducting quantum interference device (SQUID).

III. RESULTS AND DISCUSSION

The dependence of room temperature coercivity H_{ci} on ratio z for the sintered $Sm(Co_{bal}Cu_xFe_{0.06}Zr_{0.03})_z$ magnets ($x=0.08$, 0.10, and 0.12) is shown in Fig. 1. In all three samples, the coercivities significantly increase with the ratio z. For the samples with 0.10 Cu and 0.12 Cu, by increasing the ratio z from 5.8 to 7.2, the coercivities vary from 5.5 to about 40 kOe, while the coercivity of the 0.08 Cu sample changes from 1.5 to 23.6 kOe. At fixed z, the higher the Cu content, the higher the coercivity is. For the magnets with $z=5.8$, by increasing the Cu content from 0.08 to 0.12, the coercivities increase from 1.5 to 5.5 kOe, while for those with $z=7.2$, the coercivities increase from 23.6 to 40 kOe. The Cu content has a stronger effect on coercivity at higher z than at lower z. Basically, the coercivity is more sensitive to the ratio z than to the Cu content.

All the sintered magnets showed similar cellular and lamellar structures. The $Sm_2(Co,Fe)_{17}$ rhombohedral matrix is surrounded by a Cu-rich $Sm(Co,Cu)_5$ cell boundary phase, while the Zr-rich lamella phase is superimposed on the cellular microstructure. At a fixed z value, the samples with different Cu contents show a similarity in both phase structure and morphology. For a fixed Cu content, z has a strong effect on the morphology. Figure 2 shows the microstructure of samples with different z values. By increasing z from 5.8 to 7.2, the cell size varies dramatically from 10 to 80 nm, while the lamella phase density slightly increases. The samples with lower z tend to be inhomogeneous in the cell structure. Figure 3 shows the TEM data from samples with different z and Cu contents. The cell size was found to be more sensitive to z than to the Cu content. Both z and the Cu content show a smaller effect on the lamella phase density. The cell boundary thickness, which is about 8–10 nm in all samples, is not affected by either the z value or the Cu content.

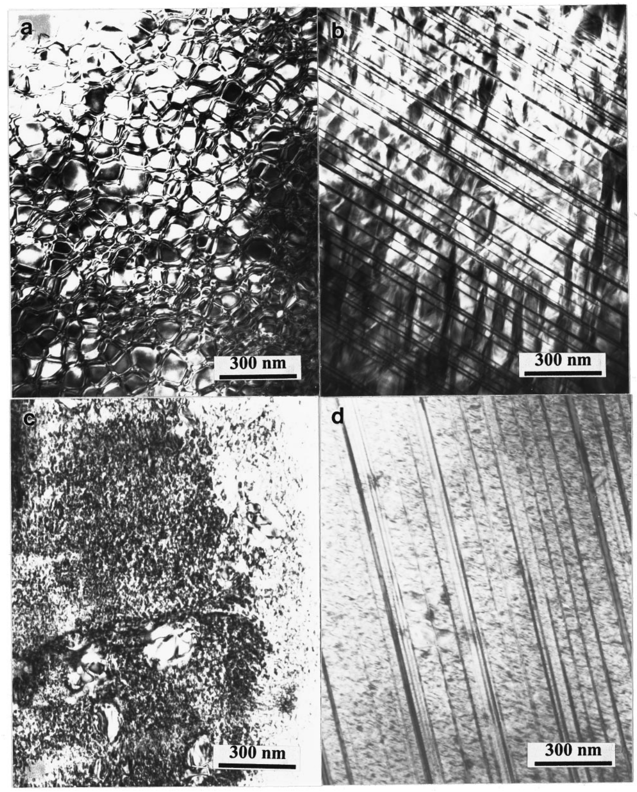

FIG. 2. TEM microstructure of sintered $Sm(Co_{bal}Cu_{0.12}Fe_{0.06}Zr_{0.03})_z$ magnets: (a), (b) $z=7.2$, cellular and lamellar structures, respectively; (c), (d) $z=5.8$, cellular and lamellar structures, respectively.

Two typical domain wall pinning sites are observed in the present study using the Fresnel and Foucault modes of Lorentz imaging. The major one is the pinning at the 1:5 cell boundaries (Fig. 4) that shows zigzag domain walls along the cell boundaries. Another, occasional pinning site, is at the intersection between the lamella phase and the cell boundary (Fig. 5). The possibility of another feature in the vicinity of this site, which is not clearly observed because of lack of resolution, cannot be excluded.

Figure 6 shows the domains and domain walls in the samples with different z. Domain walls can be pinned by cell

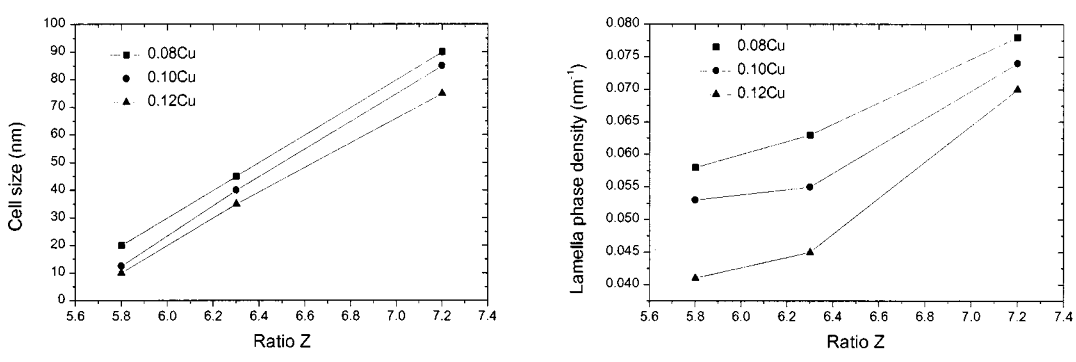

FIG. 3. TEM data of sintered $Sm(Co_{bal}Cu_xFe_{0.06}Zr_{0.03})_z$ magnets with different z and Cu contents.

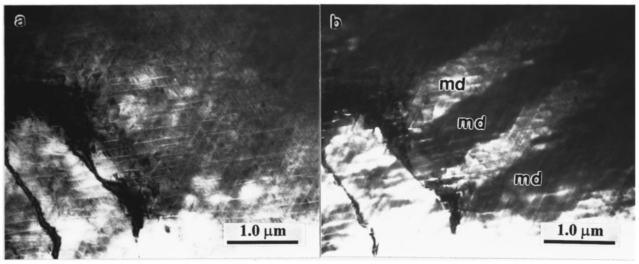

FIG. 4. Typical 1:5 cell boundary pinning in sintered $Sm(Co_{bal}Fe_{0.06}Cu_{0.10}Zr_{0.03})_{7.2}$ magnets: (a) in-focus image showing the cellular structure; (b) Foucault mode image showing magnetic domains.

boundaries and cell boundary/lamella intersections, irrespective of the cell size. The lower the ratio z, the smaller the cell size, and the less wavy the domain walls (DWs) and pinning sites are, and therefore the lower the coercivity.

These pinning sites are observed in all the samples studied. The strength of the pinning sites phase can be easily understood by considering the domain wall energy involved. In order to minimize the domain wall energy and the magnetostatic energy, domain walls must be almost parallel to the c axis. When a magnetic field is applied, the domain walls move, and the positions with the lowest average domain wall energy will be the pinning sites. The strength of the pinning sites is due to the large difference between the domain wall energies of the Cu-substituted 1:5, z and 2:17 phases. The domain wall energy for the 2:17 phase is 35 mJ/m^2 and for the 1:5 phase is 67 mJ/m^2.[7] The domain wall energy of the lamella phase at the intersection site is as low as 4–11 mJ/m^2. Our nanoprobe results revealed that Cu is concentrated in the cell boundary phase, while Zr is mainly distributed in the lamella phase.[8] The decrease in magnetic anisotropy of 1:5 caused by the increased Cu content changes in the cell boundaries leads to a lower 1:5 domain wall energy. The large domain wall energy gradient along the boundaries increases the domain wall pinning strength and therefore the coercivity. This is reason why the coercivity increases with increasing Cu content without changing the morphology and phase structure. At higher z, the cells are bigger and the amount of 1:5 smaller. For a fixed Cu content this amounts to an increased Cu content at higher z, a larger domain wall energy gradient, and therefore a larger H_{ci}.

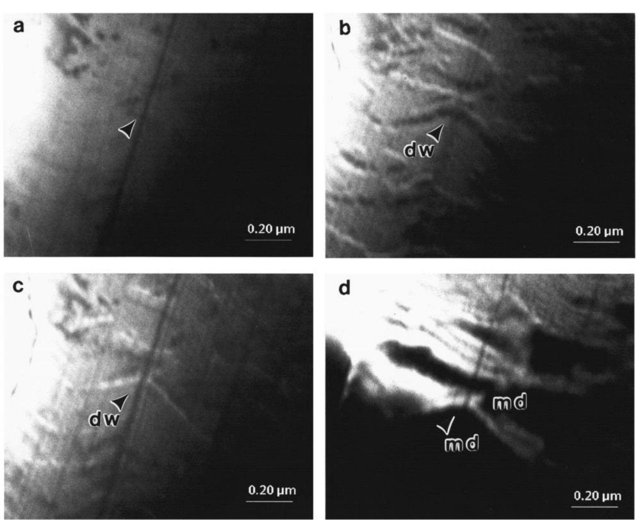

FIG. 5. Pinning sites at the intersection between the cell boundary and the lamella in sintered $Sm(Co_{bal}Fe_{0.06}Cu_{0.12}Zr_{0.03})_{6.3}$ magnets: (a) in-focus image; (b) defocus image; (c) overfocus image; (d) Foucault image.

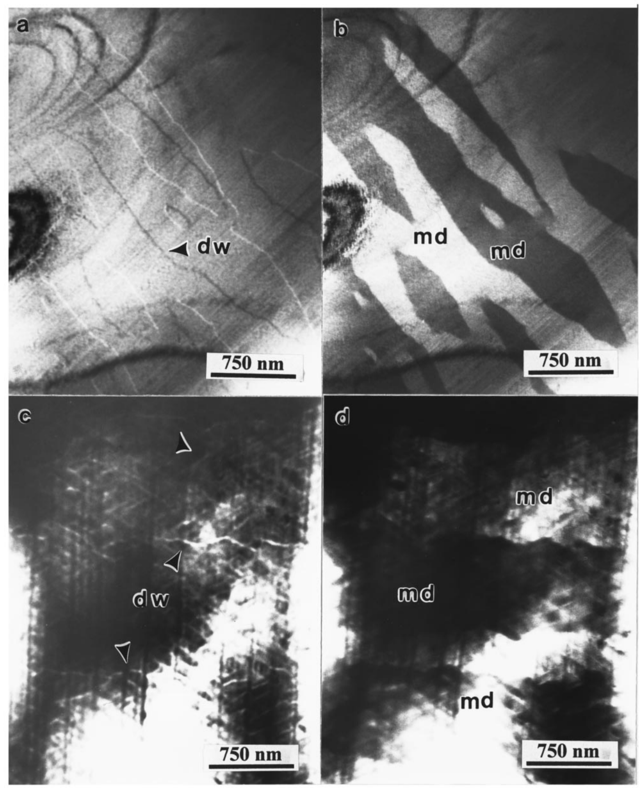

FIG. 6. Lorentz images in $Sm(Co_{bal}Cu_{0.12}Fe_{0.06}Zr_{0.03})_z$ with different ratios z: (a), (b) Fresnel mode images for $z=5.8$ and 6.3, respectively; (c), (d) Foucault images for $z=5.8$ and 6.3, respectively.

ACKNOWLEDGMENTS

This work was supported by Air Force Office of Scientific Research under Grant No. MURI F49620-96-1-0434. The authors want to thank C. Nelson for his help in the Lorentz imaging experiment at Lawrence Berkeley National Laboratory.

[1] K. Kumar, J. Appl. Phys. **63**, R13 (1988).
[2] G. C. Hadjipanayis, R. C. Hazelton, K. R. Lawless, and L. S. Horton, IEEE Trans. Magn. **18**, 1460 (1982).
[3] A. E. Ray, J. Appl. Phys. **55**, 2094 (1984).
[4] J. Fidler, J. Magn. Magn. Mater. **30**, 58 (1982).
[5] K.-D. Durst, H. Kronmuller, and W. Ervens, Phys. Status Solidi A **108**, 705 (1988).
[6] B. Y. Wong, M. Willard, and D. E. Laughlin, J. Magn. Magn. Mater. **169**, 178 (1997).
[7] M. Katter, J. Weber, W. Assmus, P. Schrey, and W. Rodewald, IEEE Trans. Magn. **32**, 4815 (1996).
[8] Y. Zhang, W. Tang, and G. C. Hadjipanayis, MURI research report, University of Delaware, 1999.